

THE UNIVERSITY OF MICHIGAN  
INDUSTRY PROGRAM OF THE COLLEGE OF ENGINEERING

COUPLED FLOW PHENOMENA IN CLAY-WATER SYSTEMS

Donald H. Gray

November, 1966

IP-756

## COUPLED FLOW PHENOMENA IN CLAY-WATER SYSTEMS

Donald H. Gray<sup>(1)</sup>

### Abstract

A thermodynamic account is given of electrokinetic and thermal coupling phenomena. A theoretical equivalence between coupling phenomena (Onsager's principle) is discussed. This equivalence was investigated experimentally for the electrokinetic case and was shown to be generally valid in clay-water systems. This means that streaming potential data on clays can be used to predict their electro-osmotic behavior.

The coupled flows of water, heat, and electricity in saturated clays were experimentally evaluated as the water content, exchange capacity, and pore water electrolyte concentration were systematically varied. A linear relationship was observed between the electro-osmotic water transport (in gallons/ampere-hr or moles/Faraday) and the logarithm of the water content.

The clay-water systems exhibited characteristic thermoelectric and thermo-osmotic coupling effects. Thermoelectric currents on the order of 1-10 microamperes/°C/cm were measured. Thermo-osmotic pressures were detected, but their importance was secondary compared to electro-osmotic contributions to the flow of water in saturated clays.

---

(1) Assistant Professor of Civil Engineering, University of Michigan, Ann Arbor, Michigan

## INTRODUCTION

Flows of matter or energy are usually described by simple laws which relate the fluxes directly to their conjugated driving forces. Darcy's and Ohm's Law are typical examples. The former describes the flow of water through the ground under a pressure gradient and the latter, the flow of electricity under an imposed voltage.

Coupling or interference effects arise when a driving force of one kind gives rise to a flow of another. A thermocouple, for example, is a device in which an electrical current is induced by an applied temperature gradient. Other lesser known, but perhaps equally interesting coupling effects can also be cited, e.g., electro-osmosis, streaming potential, and diffusion potentials.

Conventional flow processes and their coupling or interference effects are schematically illustrated in Table I. The driving forces are listed across the top, and the fluxes vertically down one side. The transport phenomena associated with various force-flux combinations are represented in a matrix in the middle. The diagonal terms running from the top left hand corner to the bottom right corner are the conjugated or conventional flow processes, described by Darcy's, Ohm's Law, etc. The off-diagonal terms are the coupling phenomena such as electro- and thermo-osmosis.

It is interesting to note from Table I that there are contributions to a given flux from sources other than the conjugated driving force. In many practical or short term applications coupling contributions to a given flux can reasonably be disregarded; in other cases, coupling properly should be taken into account. Consider for example the

TABLE I  
COUPLED FLOW PHENOMENA

| Force / Flow | Pressure Gradient                     | Temperature Gradient               | Electric Field                     | Chemical Gradient                 |
|--------------|---------------------------------------|------------------------------------|------------------------------------|-----------------------------------|
| Fluid Flow   | Darcy's Law<br>hydraulic conductivity | thermo-osmosis                     | electro-osmosis                    | normal osmosis                    |
| Heat Flow    | isothermal heat transfer              | Fourier's Law<br>heat conductivity | Peltier effect                     | Dufour effect                     |
| Current Flow |                                       | thermo-electricity                 | Ohm's Law<br>electric conductivity | diffusion and membrane potentials |
| Ion Flow     | streaming current                     | Soret effect<br>thermal diffusion  | electrophoresis                    | Fick's Law<br>diffusivity         |

situation in a geologic basin where thermal, electrical, hydrodynamic, and chemical gradients may co-exist. Coupling effects at first may seem insignificant, but over the immensity of geologic time the contribution of any one of these gradients to, let us say, fluid movement or salt accumulation in the basin may be important.

Some specific instances or applications of coupling effects in the earth are worth citing. In electric logging work a so called 'self potential' is generated by salt concentration differences between the drilling mud in a borehole and connate water in the surrounding formation. There may be a second contribution to this potential generated by the forced convection of drilling mud filtrate across the mud cake plastered on the walls of the borehole (this is known as a streaming potential). Thermo-electric potentials or currents can be induced if the reference electrode at the surface and the measuring electrodes in the borehole are at two different temperatures as a result of geothermal gradients. Shale formations can act as semi-permeable membranes and hence salt concentration differences across a shale member may produce large osmotic pressure differences. These osmotic pressures have been suggested (Berry and Hanshaw, 1960) as a possible cause of anomalous fluid pressures in the earth, i.e., deviations from the normal hydrostatic gradient with depth. Applied electrical gradients will cause a significant flow of water through certain soils, and this fact has been used successfully by engineers to dewater and stabilize water-logged ground (Cassagrande, 1953). Water movement associated with thermal gradients is important in ice lense formation and frost heaving. Thermo-osmosis has been observed and studied quite extensively in unsaturated soils; a system of particular interest to agronomists.

The present study deals with two such coupling phenomena, viz., electrokinetic and thermal coupling in clay-water-electrolyte systems. The experimental investigation reported herein was restricted to fully saturated, sodium clays. The clays varied from slurries to very stiff pastes. Highly consolidated, low water content clays with shale-like properties were not considered in the experimental study, although the same theoretical considerations should still apply.

Thermal coupling and electrokinetic effects were experimentally evaluated in several clay-water systems as the exchange capacity, water content, and concentration of pore water electrolyte were systematically varied. Irreversible thermodynamics was used as a theoretical framework for the description of the coupled flows of matter and energy in the present study.

APPLICATION OF IRREVERSIBLE THERMODYNAMICS  
TO TRANSPORT PHENOMENA

General

The theory of irreversible or non-equilibrium thermodynamics is a convenient means of analyzing the simultaneous flows of water, heat, and electricity in porous media. A detailed account of the theory is outside the scope of the present paper; furthermore, the subject is treated in depth elsewhere in this symposium.

Comprehensive treatises on the thermodynamics of irreversible processes have been written by Denbigh (1951), Prigogine (1961), Fitts (1962), and De Groot and Mazur (1962). These are directed, however, towards students of theoretical physics and chemistry. On the other hand, recent monographs by Katchalsky (1965) and Taylor (1963) deal not only with the fundamentals of the theory, but they also suggest practical applications of direct interest to the scientist or engineer.

A unified treatment of mass transport in soils by a simple phenomenologic approach was suggested quite early by Winterkorn (1947, 1955). He noted a fundamental similarity between osmosis, electro-osmosis, and thermo-osmosis, and suggested a generalization of the Darcy Law to include contributions to mass transport from electrical and thermal gradients. Simultaneous flows in soils have been investigated from a similar standpoint by Taylor and Cary (1960, 1964) and Taylor (1963). These authors reported experiments in which thermal, electrical, and salt concentration gradients were impressed across saturated samples of a silt loam. Each of these gradients caused moisture movement through the soil and they also gave rise to other coupling effects.

### Thermal Coupling

Taylor and Cary (1964) have outlined a theoretical analysis based on the thermodynamics of irreversible processes for evaluating coupled flows of heat and water in continuous soil systems. Taylor (1963) also derived the following phenomenologic equation for describing the simultaneous transfer of water and heat across a discontinuous system, viz., an inert membrane or porous soil plug.

$$J_w = \frac{L_{ww}}{T} (\Delta\mu_w)_T + L_{wq} \frac{\Delta T}{T^2} \quad (1)$$

$$J_q = \frac{L_{qw}}{T} (\Delta\mu_w)_T + L_{qq} \frac{\Delta T}{T^2} \quad (2)$$

where  $J_w, J_q$  = the net fluxes of water and heat respectively  
 $\mu_w$  = the specific chemical potential of water  
 $T$  = the absolute temperature  
 $L_{ww}, L_{qq}$  = direct transfer coefficients, e.g., the hydraulic and Fourier heat conduction coefficients respectively  
 $L_{wq}, L_{qw}$  = coupled transfer coefficients

The following assumptions were made in the derivation of these equations:

1. There is only single component flow of matter, viz., pure water.
2. The system is inert and no chemical reactions occur within it
3. External force fields are absent or cancel out.
4. The system is never too far from equilibrium, i.e.,  
 $\Delta\mu_w \ll RT$  and  $\Delta T \ll T$ .
5. Linearity exists between forces and fluxes.



The derived equations are in finite difference form, i.e., they have been integrated over the thickness of the membrane or porous soil plug. This is not as rigorous a formulation as is it when the phenomenologic equations are left in differential form. In this latter case, the driving forces are usually expressed as gradients and the flows are defined only locally at a point within the system (Taylor and Cary, 1964). The finite difference form is probably more useful for experimental purposes. It assumes, however, that suitable 'averages' can be found for the coefficients,  $L_{ik}$ , and the temperature,  $T$ , within the temperature interval,  $\Delta T$ , of interest.

The chemical potential of water  $\Delta\mu_w$  can be evaluated from the Gibbs potential for water, viz.,

$$\Delta\mu_w = -s_w \Delta T + v_w \Delta P + \sum_{k=1}^n \frac{\mu_w}{c_k} \Delta c_k \quad (3)$$

where  $s_w$ ,  $v_w$ , and  $\mu_w$  are the specific entropy, volume, and chemical potential of water;  $P$  is the pressure; and  $c_k$  is the concentration of solute species 'k'. However, for pure water at constant temperature,  $\Delta c_k = \Delta T = 0$  and Equation (3) simplifies to

$$(\Delta\mu_w)_{T, c_k} = v_w \Delta P \quad (4)$$

Substitution of  $(\Delta\mu_w)_T$  from Equation (4) into Equation (1) and (2) yields

$$J_w = \frac{L_{ww} v_w}{T} \Delta P + L_{wq} \frac{\Delta T}{T^2} \quad (5)$$

$$J_q = L_{qw} v_w \Delta P + L_{qq} \frac{\Delta T}{T^2} \quad (6)$$

Thus, Equation (5) states that the net flux of water is the sum of two transfer processes than can occur simultaneously. The first is the flow of water that is controlled by the pressure difference,  $\Delta P$ , and the hydraulic conductivity of the soil; the second is the flow of water that is induced by a temperature difference,  $\Delta T$ .

These equations are in fact specific cases of a general relationship in irreversible thermodynamics, viz., the allowable superposition of contributions to a given flux from both conjugated and non-conjugated driving forces like. The principle of linear superposition and the force-flux relationships are expressed in mathematical shorthand by

$$J_i = \sum_{k=1}^n L_{ik} X_k \quad (i,k = 1,2,3 \dots n) \quad . \quad (7)$$

where the  $J_i$ , and,  $X_k$ , are generalized fluxes and forces respectively and the,  $L_{ik}$ , are the phenomenologic transport coefficients previously defined.

When an external temperature gradient is applied across a soil plug the system eventually tends toward a steady state condition. If a counter osmotic pressure is allowed to build up in response to a thermally induced flow of water, the net flux of water will vanish at the steady state, i.e.,  $J_w = 0$ . Under these boundary conditions Equation (5) may be written as

$$\left( \frac{\Delta P}{\Delta T} \right)_{J_w = 0} = \frac{-L_{wq}}{L_{ww} V_w T} = \frac{-Q^*}{V_w T} \quad (8)$$

where  $Q^*$  is the so called 'heat of transfer'. Equation (8) indicates that the excess of pressure (the thermo-osmotic pressure) that will build up on the hot (or cold side) of a system in response to a unit temperature

difference,  $\Delta P/\Delta T$ , depends on the heat of transfer,  $Q^*$ , the specific volume of water,  $v_w$ , and the average temperature of the system,  $T$ . The heat of transfer in turn is a function of the physical properties of a membrane or porous plug. In general  $Q^*$  increases with decreasing pore size and increasing temperature.

At present there are no a priori grounds for predicting the sign of  $Q^*$ , in saturated systems, i.e., which direction the thermally induced flow of water will take. The exact mechanism of coupling between matter and heat flows is not well understood. The idea of an energetic separation, i.e., preferential passage of hot or cold molecules has been advanced by Spanner (1954). In unsaturated systems a net flow of water to the cold side has always been observed. This is understandable because of the dominant role of vapour phase transport which occurs towards the cold side. However, a simultaneous return flow of liquid water to the hot side has been observed in some cases (Krischer and Rohnalter, 1940; Taylor and Cavazza, 1954). In experiments with saturated systems using cellophane (Haas and Steinert, 1959) and silty soils (Taylor and Cary, 1960; Habib and Soeiro, 1957) a flow of water to the cold side has been reported.

One of the purposes of the present study was to determine not only the magnitude of thermo-osmotic coupling in saturated clay-water-electrolyte systems but also the direction. A clay-water system is much more complex because one is no longer dealing with an inert, single component system. Applied thermal gradients will now give rise to thermo-electric and secondary electro-osmotic effects. The possibility of thermally induced activity gradients in the pore water should also be

considered. Non-equilibrium thermodynamics provides a framework in which to consider all these possibilities, however, a theoretical treatment is omitted here. The interested reader is referred to an earlier study by Gray (1966). In the present paper only the results of experimental tests and a brief interpretation will be given.

Phenomenologic equations which describe thermo-electric coupling effects can likewise be derived (Katchalsky, 1965). Electrical effects associated with thermal gradients become important in charged membranes saturated with electrolyte solutions. Thermoelectric potentials on the order of 0.05 mv/deg°C have been reported by Ikeda (1958) for dilute KCl solutions and a cation selective collodion membrane. The warmer side had a positive polarity. Thermoelectric potentials with a typical value of 0.3 mv/deg°C for sandstones and shales have been reported by Madden and Marshall (1959). They did not give the polarity of their potentials. Taylor and Cary (1960) and Habib and Soeiro (1957) also detected small currents in their thermal coupling experiments. However, neither of these latter investigators made provision for use of suitable electrodes nor were the test conditions well suited for the detection and evaluation of thermoelectric effects.

#### Electrokinetic Coupling

Electrokinetic processes in porous media can also be characterized by phenomenologic equations. Lorenz (1952, 1953) and Goldshtein (1959) used this approach to describe electro-osmosis in clays under isothermal conditions. Both these investigators postulated that when transport of liquid and electric charge occur simultaneously, both processes combine

by simple addition in the following manner

$$J_v = L_{ww}\Delta P + L_{we}\Delta E \quad (9)$$

$$I = L_{ew}\Delta P + L_{ee}\Delta E \quad (10)$$

where

$J_v$  = the total volume flux of solution

$I$  = electric current

$\Delta P$  = pressure drop across membrane of plug

$\Delta E$  = voltage drop across membrane or plug

$L_{ik}$  = the phenomenologic transport coefficients

Equations (9) and (10) allow a contribution to either the volume flux or electric current from both a hydraulic gradient and an electric field. Again these equations are but specific cases of the general phenomenologic relationships stated earlier (Equation 7).

Katchalsky (1965) has given a rigorous derivation of the phenomenologic equations for electrokinetic processes. He starts by analyzing the individual, microscopic flows of anion, cations, and water across a membrane or porous plug. Katchalsky transforms his equations by writing them in terms of macroscopic flows of volume, current, and diffusion flux. This is a permissible and much more practical formulation for experimental purposes.

In the classic electrokinetic case it is necessary to assume that no significant ion concentration gradients develop, and therefore that no osmotic counter pressure can develop. This is a critical assumption in the case of electro-osmosis experiments because the prolonged application of a high density D.C. current must inevitably cause electrolyte

accumulation on one side of a membrane and depletion on the other (Miller, 1955). Careful attention to experimental detail or at least an awareness of this complication is required to avoid misinterpretation of electro-osmosis data.

High current density may also lead to instability in the phenomenologic coefficients and non linear effects, particularly if the current tends to alter the fabric and flow geometry of the medium. The effect of an applied current on the hydraulic conductivity can be analyzed better by re-arranging Equation (9) in slightly different form. The single action coefficient,  $L_{ww}$ , is defined when all forces except the pressure gradient are zero. However, the usual procedure when measuring hydraulic permeability is under open circuit conditions, viz  $I = 0$ ,  $\Delta E \neq 0$ . In this case a more convenient phenomenologic equation can be introduced for the volume flux,  $J_v$ , in terms of a modified electro-osmotic coefficient,  $\beta$ , and a hydraulic filtration coefficient,  $K$ , measured under open electrical circuit conditions. Thus

$$J_v = K\Delta P + \beta I \quad (11)$$

where

$$K = \left( \frac{J_v}{\Delta P} \right)_{I=0} = L_{ww} - \frac{L_{ew}L_{we}}{L_{ee}} \quad (12)$$

$$\beta = \left( \frac{J_v}{I} \right)_{\Delta P=0} = \frac{L_{ew}}{L_{ee}} \quad (13)$$

Note that  $K$  and  $L_{ww}$  are equal only if one of the coupling coefficients,  $L_{ew}$  or  $L_{we}$ , is zero.

A graphical plot of the generalized flow Equation (11) is shown schematically in Figure 1. All plots are linear and are drawn with the same slope. A constant slope for different current intensities

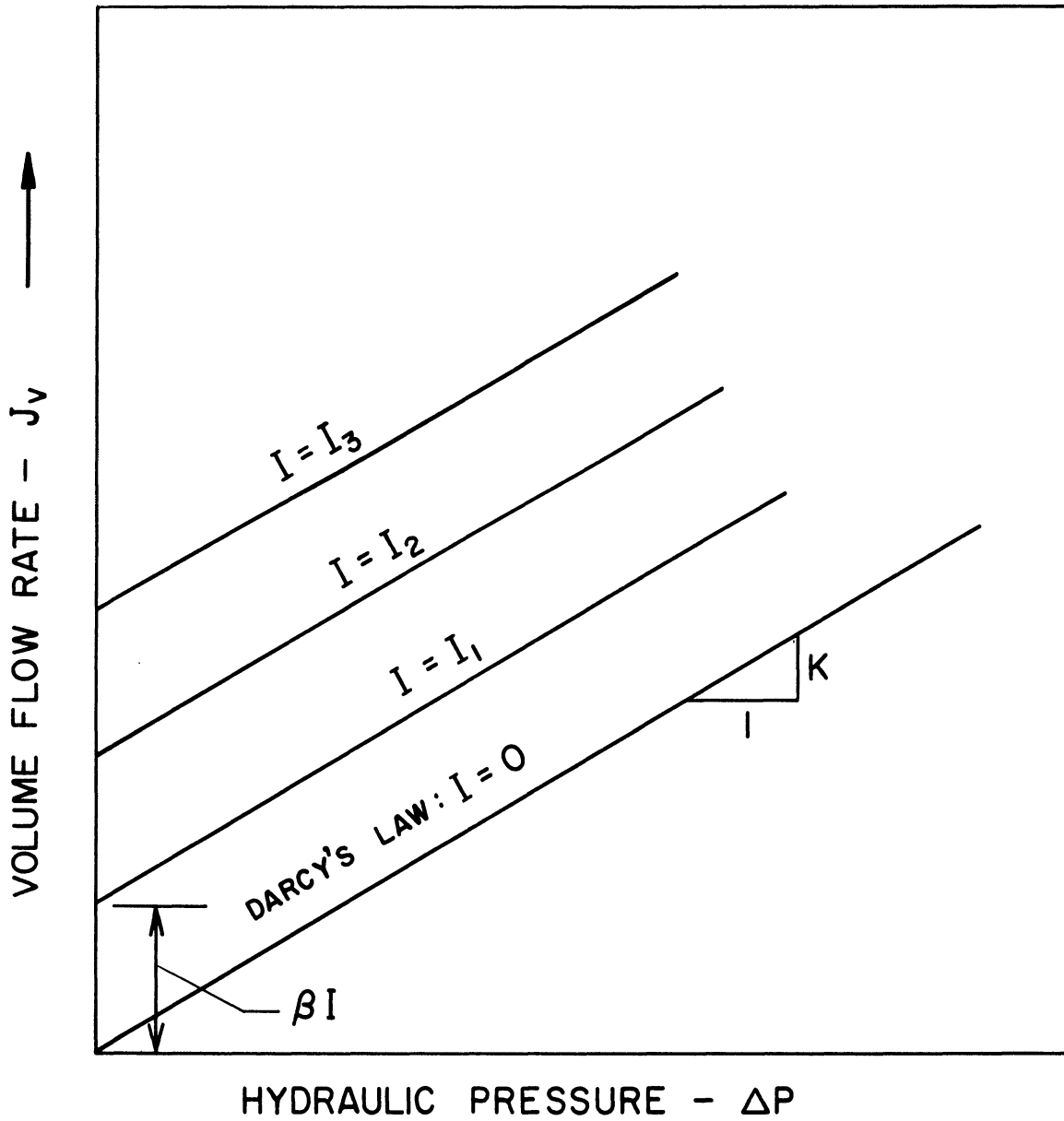


Figure 1. Graphical Representation of Equation (11) Showing Electrical Contribution to Volume Flow.

has an important physical significance, viz., that the passage of a D.C. current is not altering the flow geometry of the porous medium. Prolonged passage of a high intensity D.C. current in one direction will tend to cause physico-chemical changes, at least in a clay-water system, and thus produce non-linear effects. Effects such as these during electro-osmosis experiments in clays have been reported by Casagrande (1949), Goldshtein (1959), and Cambefort (1961). On the other hand, certain experimental precautions (to be outlined later) will eliminate these problems. Olsen (1965), for example, has established the validity of Equation 11 for a kalinite-water system over a wide range of water contents.

A very interesting and useful equivalence can be derived for matter flowing in response to an applied electrical field and electric charge flowing in response to an applied pressure gradient. Saxen (1892) first established this relationship experimentally by observing an equivalence between electro-osmosis and streaming potential phenomena in clay diaphragms. This equivalence has subsequently become known as Saxen's Law. However, a much more general proof of Saxen's Law can be established from symmetry relations between coupling coefficients.

Symmetry relations between coupling coefficients were derived by Onsager (1931) and they largely form the cornerstone of the modern theory of non-equilibrium thermodynamics. Onsager's fundamental theorem states that provided a proper choice is made of the fluxes,  $J_i$ , and forces,  $X_i$ , all the coefficients,  $L_{ik}$ , with  $i \neq k$  must satisfy the equality

$$L_{ik} = L_{ki} \quad (i, k = 1, 2, 3, \dots, n) \quad (14)$$



The equalities expressed in Equation (14) form an important link between the various coupling phenomena. Miller (1960) has reviewed experimental verifications of Onsager's symmetry relations and has shown them to be valid for a wide class of coupling phenomena including electrokinetic coupling.

Saxen's Law can thus be proved theoretically by applying Onsager's symmetry relations to the phenomenologic equations describing electrokinetic phenomena. If the boundary conditions for a hypothetical electro-osmosis and streaming potential experiment are substituted in Equations (9) and (10), the following identities are obtained.

Case i) Streaming Potential Experiment ( $I = 0$ )

$$\left( \frac{\Delta E}{\Delta P} \right)_{I = 0} = - \frac{L_{we}}{L_{ee}} \quad (15)$$

Case ii) Electro-osmosis Experiment ( $\Delta P = 0$ )

$$\left( \frac{J_v}{I} \right)_{\Delta P = 0} = \frac{L_{ew}}{L_{ee}} \quad (16)$$

Saxen demonstrated experimentally that the terms on the left hand side of Equations (15) and (16) are equal to one another, i.e.,

$$\left( \frac{\Delta E}{\Delta P} \right)_{I = 0} = - \left( \frac{J_v}{I} \right)_{\Delta P = 0} \quad (17)$$

However, this equivalence must also follow from the thermodynamic considerations if Onsager's symmetry condition is valid, i.e. if

$$L_{ew} = L_{we} \quad (18)$$

The practical utility of this equivalence can be demonstrated for the electrokinetic case. It means, for example, that existing streaming potential data could be used to predict electro-osmotic behavior. This is quite significant in view of the scarcity of extensive electro-osmosis data in clay-water-electrolyte systems and the difficulty in making an electro-osmotic measurement. Furthermore, considerable streaming potential data is already available. Olsen (1961), for example, has measured streaming potentials in homionic and natural clays over a wide range of water contents and external electrolyte concentrations. In principle his data can be used to predict electro-osmosis in clays providing, of course, that the Saxon relations are generally valid in clay-water systems. In practical units the Saxon relation (Equation 17) may be written as

$$\frac{\text{Moles of water}}{\text{Faraday equivalent}} = \frac{\text{Milli volts}}{\text{atmosphere}} \times 54.5 \quad (18)$$

This equivalence is examined further as part of the experimental investigation reported herein.

## EXPERIMENTAL PROCEDURE

### General

The effects of a systematic variation in certain key parameters on electrokinetic and thermal coupling processes in clay-water systems were studied. The parameters of special interest were the following:

1. Water content
2. Exchange capacity
3. Normality of the external electrolyte

Other variables, such as the type of counter-ion and the degree of saturation, were held constant by restricting the investigation to fully saturated, sodium clays. A detailed account of the experimental procedure has been given by Gray (1966); salient features are summarized below.

### Materials and Apparatus

Experimental data were obtained on three types of material: a pure kaolinite (Hydrite UF), and illitic clay (Grundite), and an artificial silty-clay comprised of equal parts by weight of kaolinite and silica flour. These clays and their properties are described in Table II.

The clays were made as nearly homoionic to sodium ion as possible by washing batches of clay in concentrated solutions of sodium chloride. The excess salt was then removed by leaching the clays with distilled water. The clays were subsequently dried in an oven at 230°F, lightly pulverized, and stored in sealed jars for further use. Weighed amounts of each clay were later mixed with the desired electrolyte

TABLE II  
 PROPERTIES AND DESCRIPTION OF TEST MATERIALS

| Descriptive Name of Test Material | Proprietary Name | Mineralogy  | Size Range     | Specific Gravity | Exchange Capacity Meq/100 gm | Supplier                                     |
|-----------------------------------|------------------|---|----------------|------------------|------------------------------|--|
| Kaolinite                         | Hydrite UF       | Kaolinite-100%  | < 2 Micron     | 2.63             | 3.8                          | Georgia Kaolin Co.                           |
| Illitic clay                      | Grundite         | 1 Illite - 55%<br>Kaol. - 10<br>Quartz - 20<br>Mixed layer - 15 | 2 <10 Micron   | 2.78             | 16.8                         | Illinois Clay Products Company               |
| Silty clay                        | None             | Kaol. - 50%<br>Silica flour - 50%                               | < No. 325 Mesh | 2.65             | 2.1                          | Gopher State Silica Inc. (silica flour only) |

Notes:

1. Based on X-ray diffraction analysis by Esrig (1964)
2. Fractionated portion of original material
3. Measured by Sanitary Engineering Research Lab., Univ. of Calif.

solution into thick slurries prior to their introduction into a specially constructed flow cell.

The flow cell itself was designed so that known thermal, electrical, and hydraulic pressure gradients could be applied across the clay samples. Provisions were made to monitor the flows of electricity and water (or solution) that resulted from the application of any one of the gradients. In some cases, it was preferable to pass a known electric current across the system and monitor the voltage drop instead. This capability was provided by a constant current D.C. power supply. A schematic diagram of the test layout is shown in Figure 2 and a general view of the flow cell and test equipment, in Figure 3a.

The flow cell was constructed entirely of lucite plastic; nylon fittings and plastic tubing were also used throughout. The sample chamber was cylindrical and had two retractable pistons with recessed porous stones at either end. An exploded view of the flow cell components is shown in Figure 3b. By placing the entire flow assembly in a loading frame as shown in Figure 3a it was possible to consolidate the clay samples and reduce their water content to predetermined levels.

Internal heating and cooling coils were installed in the piston heads in order to establish a temperature gradient across the clay sample for thermal coupling tests. The heating and cooling coils in turn were connected to external constant temperature circulators. Temperatures were monitored with thermistor probes and a digital thermometer. The flow cell and test equipment were kept in a constant temperature room maintained at 20°C.

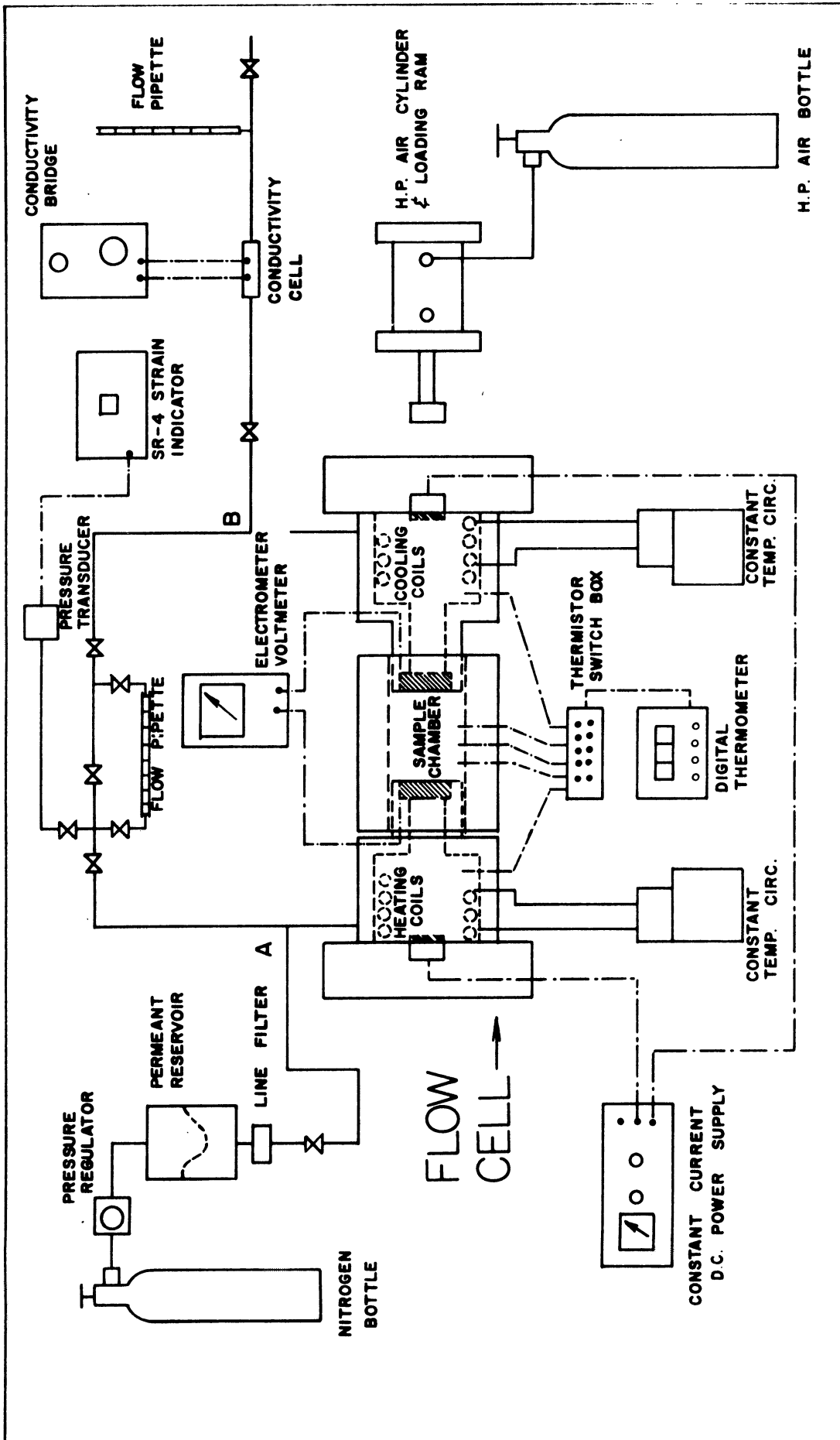
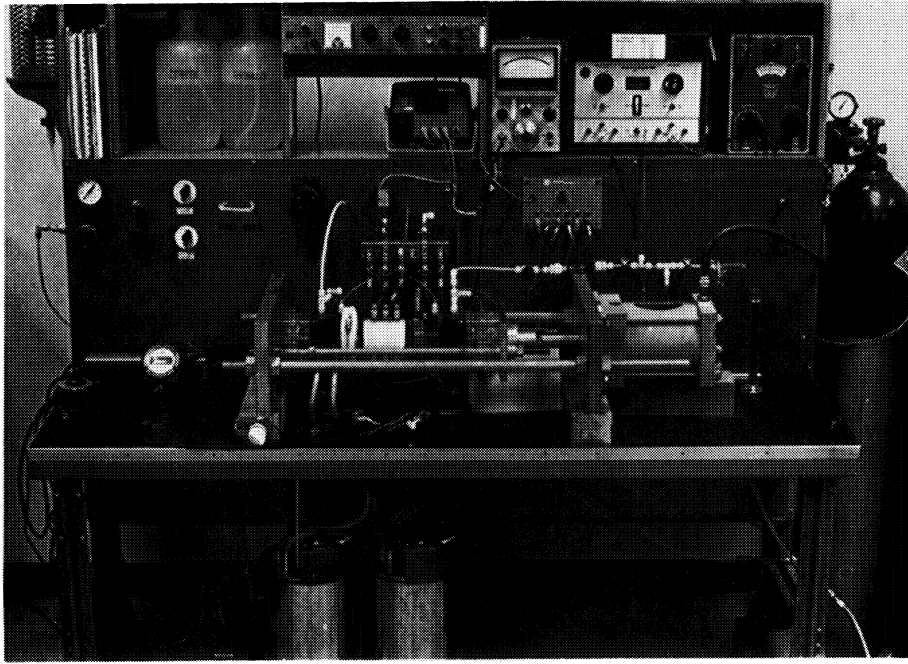
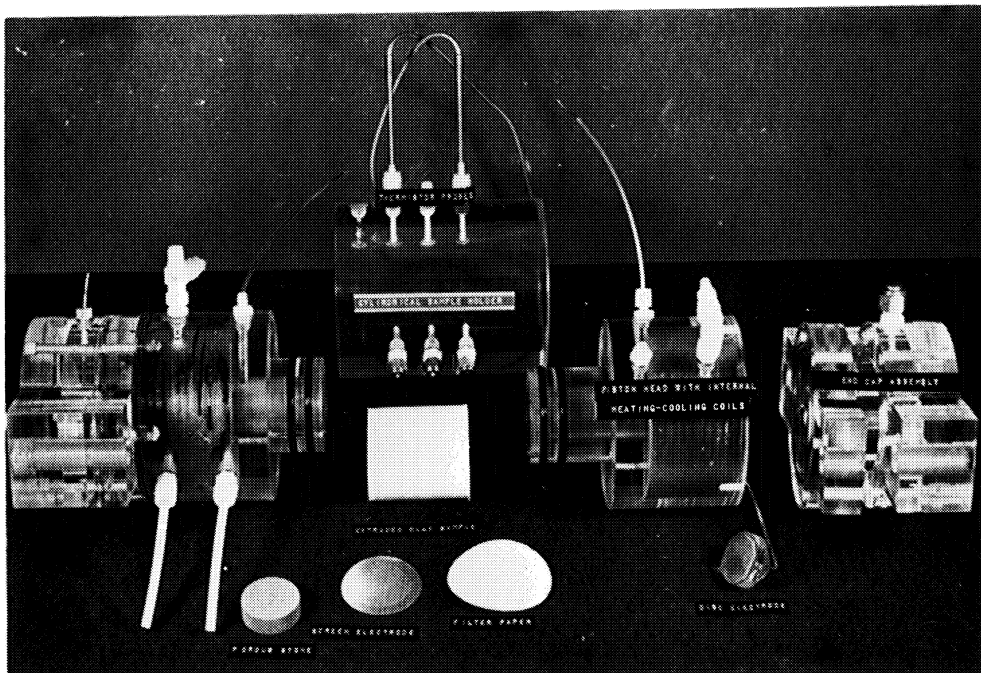


Figure 2. Schematic Diagram of Flow Cell and Test Layout.



(a)



(b)

Figure 3. General and Close Up View of Flow Cell and Test Equipment.

### Electrokinetic experiments

Four transport coefficients were determined in the electrokinetic experiments: the hydraulic permeability, electrical conductivity, electro-osmotic coefficient, and the streaming potential coefficient. The last two are equivalent if Saxon's Law or the Onsager symmetry relations are valid. The hydraulic permeability,  $K$ , is the conventional filtration coefficient measured under open electrical circuit conditions ( $I = 0$ ). The electrical conductivity was measured under conditions of no hydraulic back pressure ( $\Delta P = 0$ ). The electro-osmotic coefficient, ( $\beta$ ), is defined in the present study as the water transport per unit charge, e.g. gallons per ampere-hr. or moles per Faraday.

The hydraulic permeability was determined by measuring the flow rate through a sample under constant hydraulic head. The pressure drop across the clay sample was determined by monitoring the pressure in the solution at each end of the sample by means of an electrical pressure transducer.

The electrical conductivity was measured by passing a known current through the sample from a constant current power source. Separate electrodes were used for application of current and measurement of voltage. Both sets of electrodes were silver-silver chloride; their preparation is described by Gray (1966). The applied currents were limited to a range between 10 and 1000 micro-amps. The current was always passed in two directions through the sample and an average taken of the resulting voltage drops. This procedure tended to cancel out any asymmetry potentials that might have been present. The voltage drops across the sample were measured with a Kiethley Model 610B electrometer which could be used as either a voltmeter or ammeter.



Streaming potentials were measured by applying a known hydraulic pressure and recording the electric potential generated across the sample. In order to successfully measure streaming potentials it was necessary to use a very high impedance voltmeter so as to avoid drawing down the voltage source. This requirement is especially critical when measuring very small streaming potentials (on the order of a few millivolts in some clay samples). The Kiethley electrometer adequately satisfied this requirement because it has an input resistance (if needed) of  $10^{14}$  ohms.

Electro-osmotic transport of water (or solution) was measured by applying a known current from the constant current power source across a clay plug and observing the resulting volume flow rate of solution. The flow rate was determined by timing the movement of an air bubble in a calibrated pipette which formed part of a closed loop between the solution compartments on either side of the clay sample. By-passing of water along the walls of the pipette was prevented by water-proofing the pipette with a commercial hydrophobing agent. This treatment also produced a sharp meniscus at the air-water interface in the bubble.

Much has been written (Miller, 1955 ; Cambefort, 1961) about the effects of a prolonged application of a D.C. current across a clay-water system with respect to causing electrolysis, ion exchange, gas formation at the electrodes, physico-chemical alteration of the clays, heating, and the build up of concentration gradients across the clay plug. All of these effects were eliminated or suppressed to a negligible level in the present study by the precautions outlined below:

- a. Use of reversible silver-silver chloride current electrodes.
- b. Use of homoionic clays and a saturating solution with the same ion as the counter-ion

- c. Limitation of the current density to less than 35 microamps/cm<sup>2</sup>.
- d. Systematic reversal of the current flow direction and limitation of the duration of current flow in any one direction to less than 15 minutes.
- e. Stirring the solution on either side of the clay plug and use of relatively large volumes of solution to swamp concentration changes.

Electro-osmosis was always measured by applying the current an equal time in opposite directions and taking an average of the two runs. This procedure cancelled out secondary apparatus effects and prevented accumulation of electrolyte on one side or the other.

Because of the highly idealized testing conditions used the electro-osmotic flow rates represented upper bound or limiting values compared to those that would be observed in a field installation when such controls could not be used.

#### Thermo-osmotic and thermo-electric tests

Thermo-osmotic pressures were measured in lieu of osmotic flow rates; this procedure was adopted for experimental convenience. The standard procedure was to apply a temperature gradient across a clay sample and observe the build-up in pressure as indicated by the rise or drop of water level in standpipes on either side. The ends of the clay plug were electrically short circuited through an ammeter and the induced thermo-electric current recorded concurrently with the thermo-osmotic pressure.

Upon applying a temperature gradient the water level quickly rose in the standpipes because of an initial thermometric expansion, but the two levels equalized because the standpipes were connected by an open

bypass valve. Periodic temperature readings were taken to determine how quickly the system approached a steady-state distribution. Five hours proved to be an adequate time interval for temperature stabilization.

At the end of five hours, the bypass valve was closed and a temperature-induced pressure difference could develop across the clay plug. The pressure difference was directly proportional to the difference in water level in the two standpipes. The levels were read with the aid of a cathotometer. Periodic readings of the pressure difference were taken until an equilibrium pressure was reached. This was taken as the steady-state condition at which point the volume flow vanishes,  $J_v = 0$ . The pressure difference at this point was the thermo-osmotic pressure of interest.

Simultaneous readings of the thermo-electric current were taken also. A continuous and characteristic plot of current vs. time for each clay-water system was obtained in this manner.

## RESULTS

### Electrokinetic Coefficients

Experimental electrokinetic coefficients for the clay-water-electrolyte systems are tabulated in Tables III and IV. They include the hydraulic permeability, electrical conductivity, electro-osmotic transport, and streaming potential coefficient. Each of these coefficients was calculated from the slope of an experimental plot of 'flux' vs. appropriate 'force'. Typical plots for electro-osmotic transport and streaming potential are shown in Figures 4 and 5 for a kaolinite mixed with 0.01N NaCl solution.

Also shown in Tables III and IV is a comparison of measured electro-osmotic transport (Column 'a') and the calculated equivalent electro-osmotic transport (Column 'b'). The latter was calculated from the streaming potential data according to Saxon's Law (Equation 18).

### Thermo-osmotic and Thermo-electric Tests

Steady state thermo-osmotic pressures and thermo-electric currents are tabulated in Table V. Also shown in Table V are the temperature gradient and the mean temperature in the samples after attainment of a steady state temperature distribution. A gradient of approximately  $1^{\circ}\text{C}/\text{cm}$  and a mean temperature of about  $26^{\circ}\text{C}$  were commonly observed.

A typical thermo-osmotic pressure build up curve for kaolinite is shown in Figure 6. Steady state thermo-osmotic pressures are shown plotted vs. water content in Figure 7 for the various clay-water-electrolyte systems. Except in two instances, the pressure rise always occurred at the hot side.

TABLE III  
ELECTROKINETIC COEFFICIENTS  
IN CLAY -  $10^{-3}$  N SODIUM CHLORIDE SYSTEMS\*

| Test Number | Sample       | Water Content Percent | Permeability cm/sec x $10^7$ | Conductivity micromhos/cm | Streaming Potential mv/atmos | Electro-osmotic Transport moles H <sub>2</sub> O/Faraday | Equiv. Electro-osmotic Transport** moles H <sub>2</sub> O/Faraday | Ratio b/a |
|-------------|--------------|-----------------------|------------------------------|---------------------------|------------------------------|--|---|-----------|
| 1           | Silty Clay   | 50.1                  | 6.55                         | 54                        | -62.0                        | <sup>a</sup> 3440  | <sup>b</sup> 3370   | .98       |
|             |              | 41.9                  | 3.71                         | 48                        | -56.2                        | 3130   | 3060  | .98       |
|             |              | 32.0                  | 1.81                         | 41                        | -48.4                        | 2620   | 2640  | 1.01      |
|             |              | 23.6                  | 0.44                         | 36                        | -36.0                        | 1940   | 1960  | 1.01      |
|             |              | 19.3                  | N.R.                         | N.R.                      | N.R.                         | 1740   |   |           |
| 2           | Kaol.        | 65.4                  | 6.57                         |                           | -39.0                        | 2410   | 2130  | .88       |
|             |              | 54.9                  | 2.61                         |                           | -3.0                         | 2060   | 2020  | .98       |
|             |              | 44.4                  | 0.77                         | N.R.                      | -31.5                        | 1850   | 1720  | .93       |
|             |              | 34.4                  | 0.34                         |                           | -25.0                        | 1420   | 1365  | .98       |
|             |              | 30.4                  | 0.26                         |                           | -21.8                        | 1260   | 1190  | .94       |
| 3           | Illitic Clay | 102.0                 | 6.12                         | 1100                      | -6.2                         | 410  | 338   | .82       |
|             |              | 84.0                  | 1.27                         | 1110                      | -5.1                         | 268  | 227   | .85       |
|             |              | 59.1                  | 0.27                         | 760                       | N.R.                         | 204  |   |           |
|             |              | 43.5                  | 0.07                         | 930                       | N.R.                         | 148  |   |           |
|             |              | 37.3                  | N.R.                         | 860                       | -1.9                         | 120  | 104   | .88       |

Notes:

\* Experimental coefficients measured at 20°C

\*\* Calculated from Saxen's Law (Equation 18)

N.R. - Not Recorded

TABLE IV

ELECTROKINETIC COEFFICIENTS  
IN CLAY -  $10^{-2}$  N SODIUM CHLORIDE SYSTEMS\*

| Test Number | Sample       | Water Content Percent | Permeability cm/sec x $10^7$ | Conductivity micromhos/cm | Streaming Potential mv/atmos | Electro-osmotic Transport moles H <sub>2</sub> O/Faraday | Electro-osmotic Transport** moles H <sub>2</sub> O/Faraday | Ratio b/a |
|-------------|--------------|-----------------------|------------------------------|---------------------------|------------------------------|--|--|-----------|
| 4           | Silty Clay   | 74.0                  | N.R.                         | 497                       | - 6.7                        | <sup>a</sup> 350   | <sup>b</sup> 365   | 1.04      |
|             |              | 51.0                  | 11.6                         | 408                       | - 6.4                        | 325  | 348  | 1.07      |
|             |              | 41.4                  | N.R.                         | 334                       | - 6.1                        | 320  | 332  | 1.04      |
|             |              | 32.0                  | 2.31                         | 257                       | - 5.9                        | 310  | 332  | 1.04      |
|             |              | 26.0                  | N.R.                         | N.R.                      | - 5.7                        | 305  | 310  | 1.02      |
| 5           | Kaol.        | 73.7                  | 9.7                          | 602                       | -14.8                        | 825  | 806  | 0.98      |
|             |              | 61.7                  | 4.85                         | 563                       | -13.3                        | 766  | 725  | .95       |
|             |              | 52.2                  | 1.52                         | 504                       | -12.6                        | 707  | 686  | .97       |
|             |              | 42.7                  | 0.83                         | 436                       | -12.0                        | 653  | 654  | 1.00      |
|             |              | 33.3                  | 0.39                         | N.R.                      | -10.1                        | 568  | 550  | 0.97      |
| 6           | Illitic Clay | 98.0                  | N.R.                         | 1810                      | - 3.06                       | 214  | 167  | 0.78      |
|             |              | 78.6                  | 1.49                         | 1630                      | - 2.82                       | 161  | 154  | .96       |
|             |              | 67.0                  | N.R.                         | 1400                      | - 2.60                       | 145  | 141  | .97       |
|             |              | 56.6                  | 0.34                         | 1560                      |                              | 130  |  |           |
|             |              | 43.7                  | N.R.                         | N.R.                      | - 1.70                       | 107  | 93   | .87       |

Notes:

\* Experimental coefficients measured at 20°C

\*\* Calculated from Saxen's Law (Equation 18)

N.R. - Not Recorded

TABLE V  
 STEADY STATE THERMO-OSMOTIC AND THERMO-ELECTRIC DATA  
 IN CLAY-WATER-ELECTROLYTE SYSTEMS

| Test Number | Sample       | Permeant    | Water Content % | Thermo <sup>-1</sup> Osmotic Pressure cm H <sub>2</sub> O/°C | Thermo <sup>-2</sup> Electric Current Microamps per °C/cm | Temp. Grad. °C/cm | Mean Temp. °C |
|-------------|--------------|-------------|-----------------|--|---|-------------------|---------------|
| 1           | Silty Clay   | .001 N NaCl | 64.0            | .04  | 1.15  | 0.99              | 26.2          |
|             |              |             | 41.7            | .10  | 1.05  | 0.92              | 26.5          |
|             |              |             | 33.0            | .15  | 0.90*   | 0.98              | 26.8          |
|             |              |             | 24.4            | .18  | 0.85  | 0.96              | 27.2          |
| 2           | Kaolinite    | .001 N NaCl | 54.9            | .20  | 2.10  | .92               | 25.8          |
|             |              |             | 34.4            | .46  | 1.65  | 1.08              | 26.1          |
|             |              |             | 30.4            | .51  | 1.60  | 1.08              | 26.8          |
| 3           | Illitic Clay | .001 N NaCl | 84.0            | .05  | 2.95  | 1.00              | 26.3          |
|             |              |             | 59.1            | -.18   | 2.75*   | 1.03              | 26.0          |
|             |              |             | 43.5            | -.08   | 2.65  | 1.00              | 26.1          |
| 4           | Silty Clay   | .01N NaCl   | 51.0            | .03  | 2.60*   | 0.94              | 27.5          |
|             |              |             | 31.9            | .05  | 2.40  | 1.04              | 27.3          |
| 5           | Kaolinite    | .01N NaCl   | 73.7            | .08  | 3.85  | 0.95              | 26.0          |
|             |              |             | 52.2            | .12  | 3.45  | 0.97              | 26.4          |
|             |              |             | 42.7            | .16  | 3.20  | 0.96              | 26.2          |

Notes:  
<sup>1</sup> Negative sign indicates pressure rise at cold side  
<sup>2</sup> Polarity: hot side positive  
 \* Estimated by interpolation

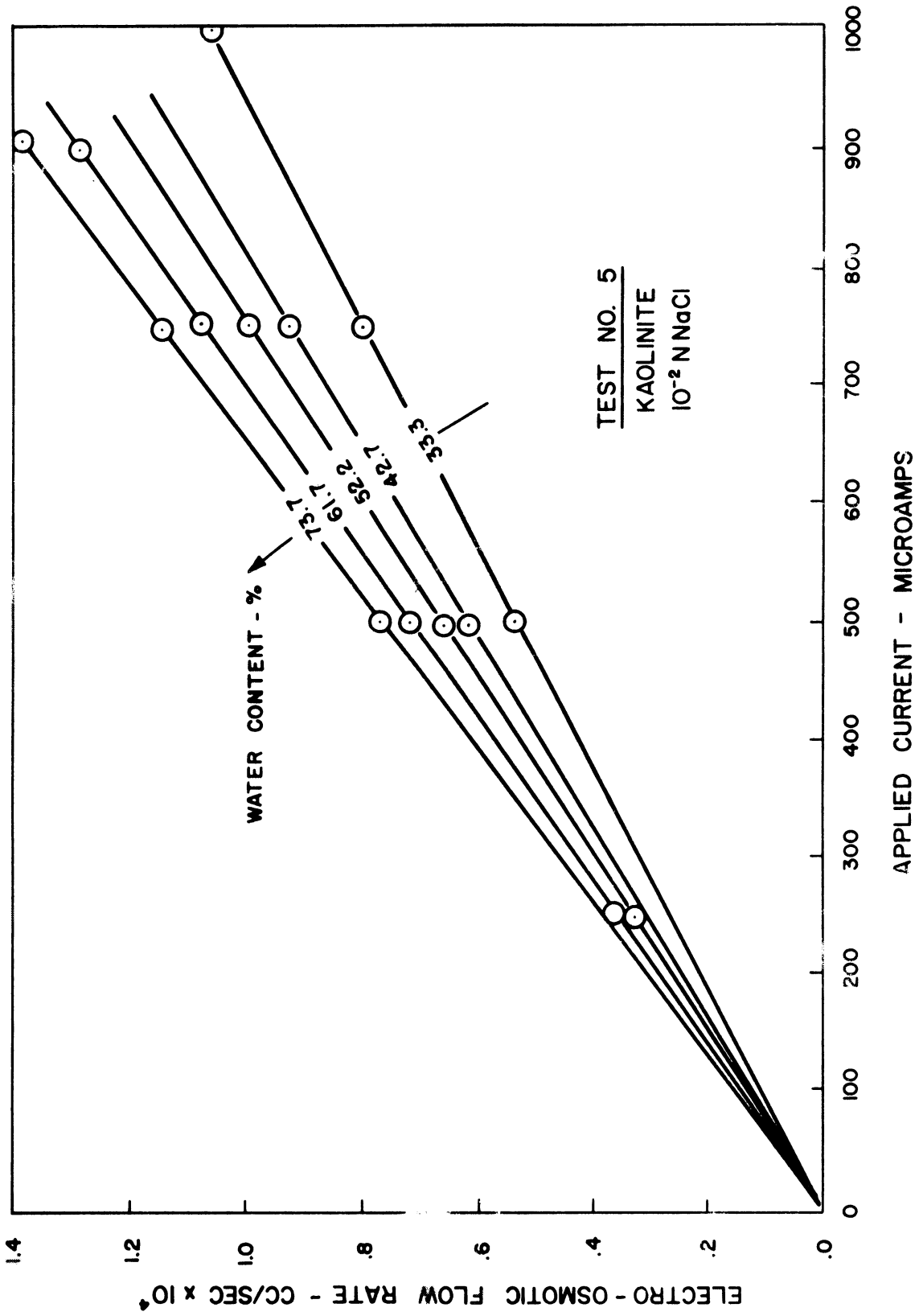


Figure 4. Electro-osmotic Flow Rate vs. Applied Current in Kaolinite.



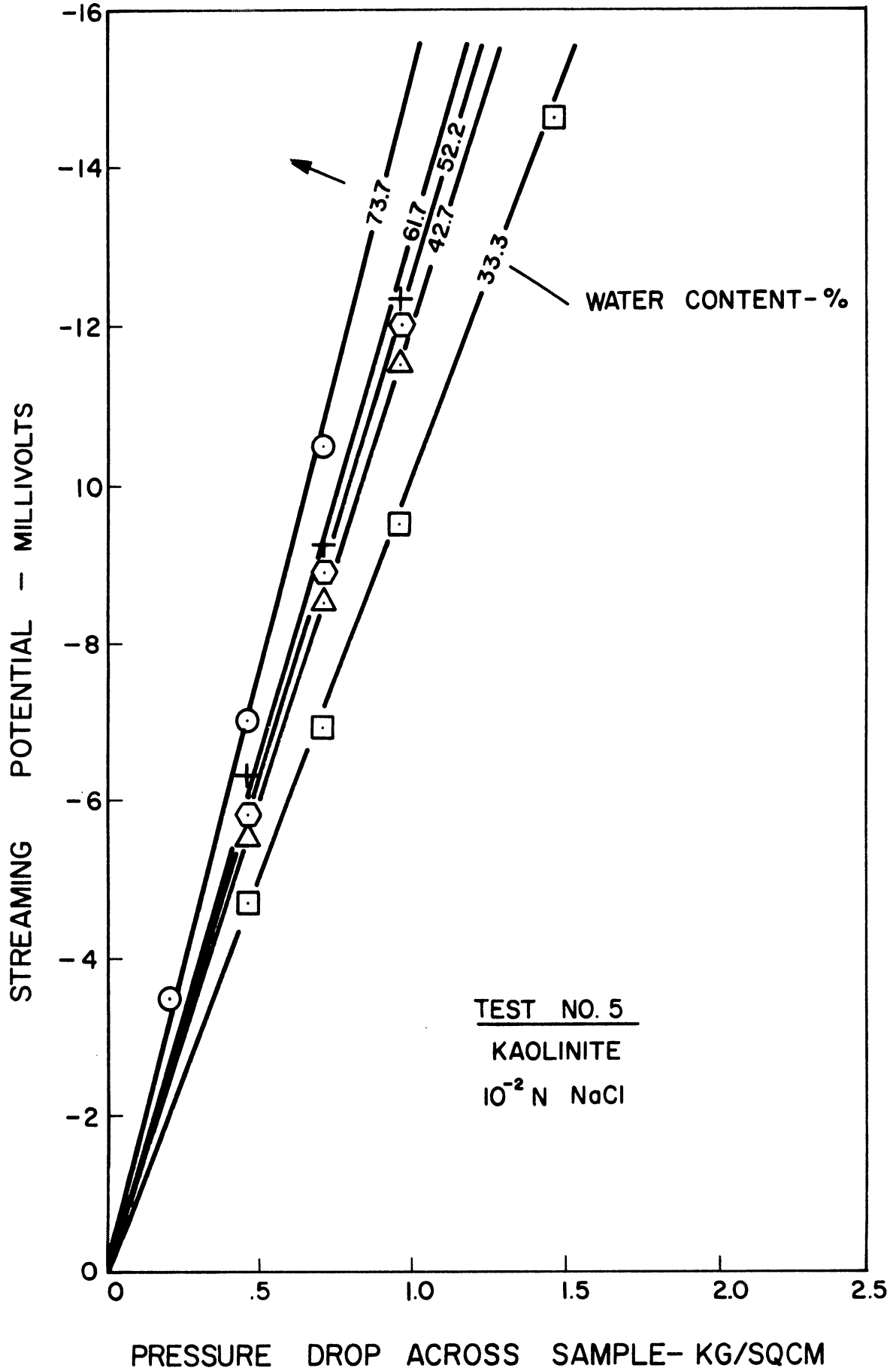


Figure 5. Streaming Potential vs. Pressure in Kaolinite.

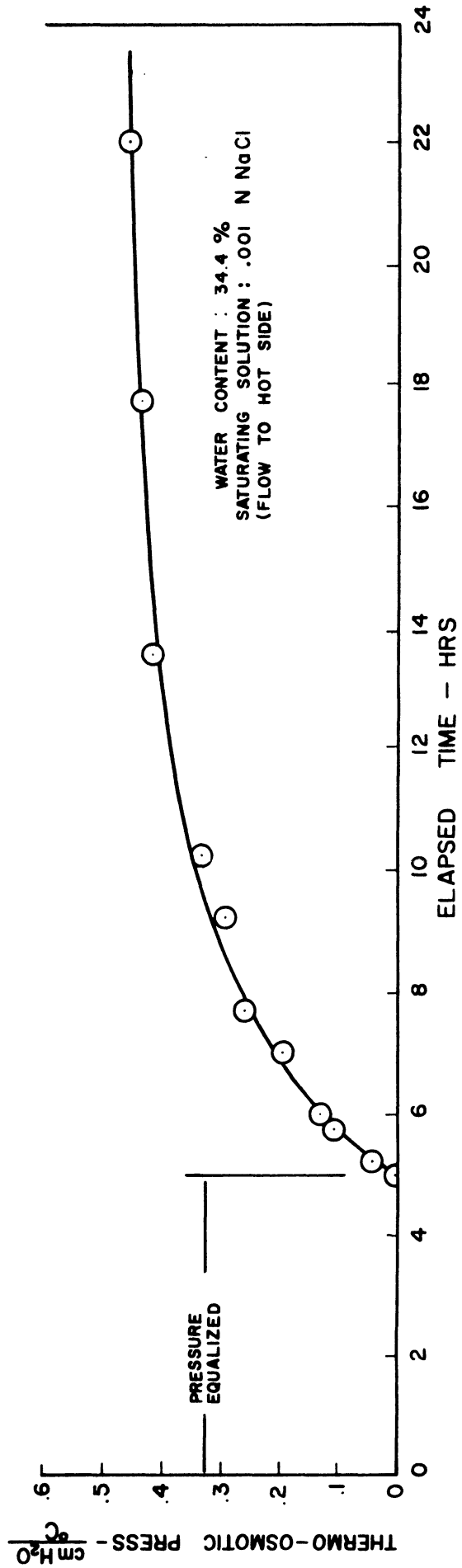
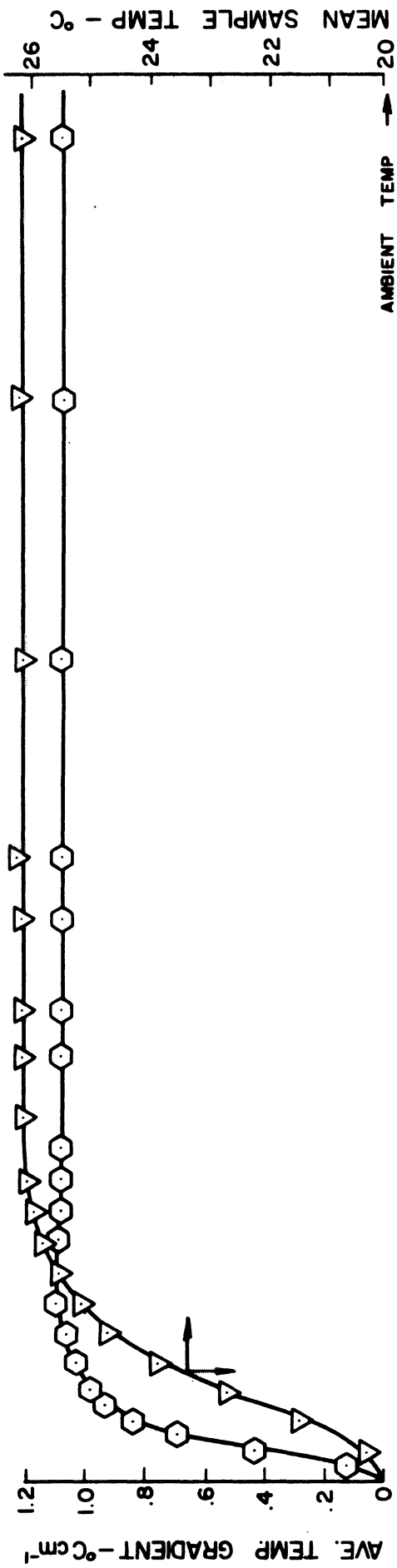


Figure 6. Thermo-osmotic Pressure Build Up in Kaolinite.

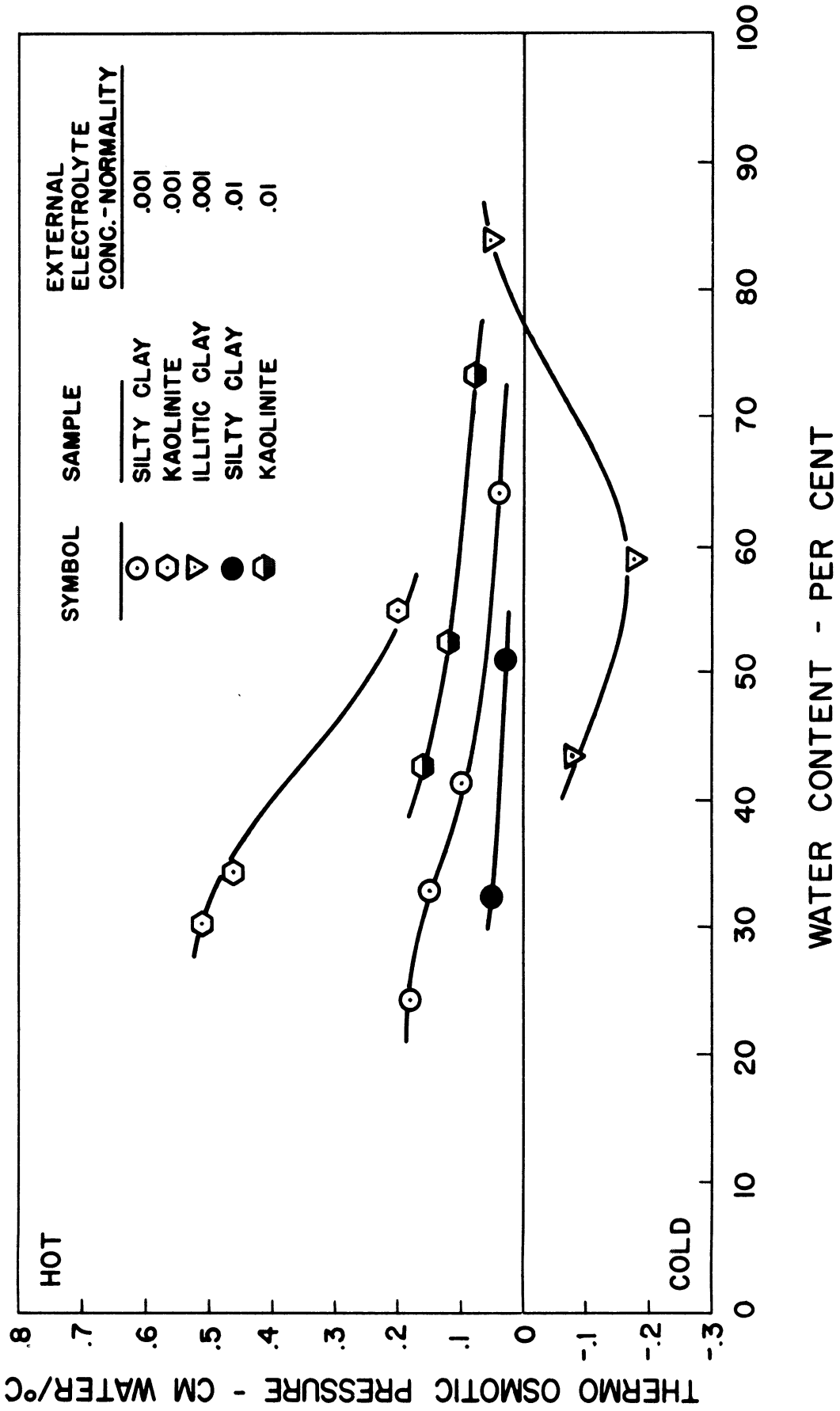


Figure 7. Thermo-osmotic Pressure vs. Water Content in Clay-Water Electrolyte Systems.

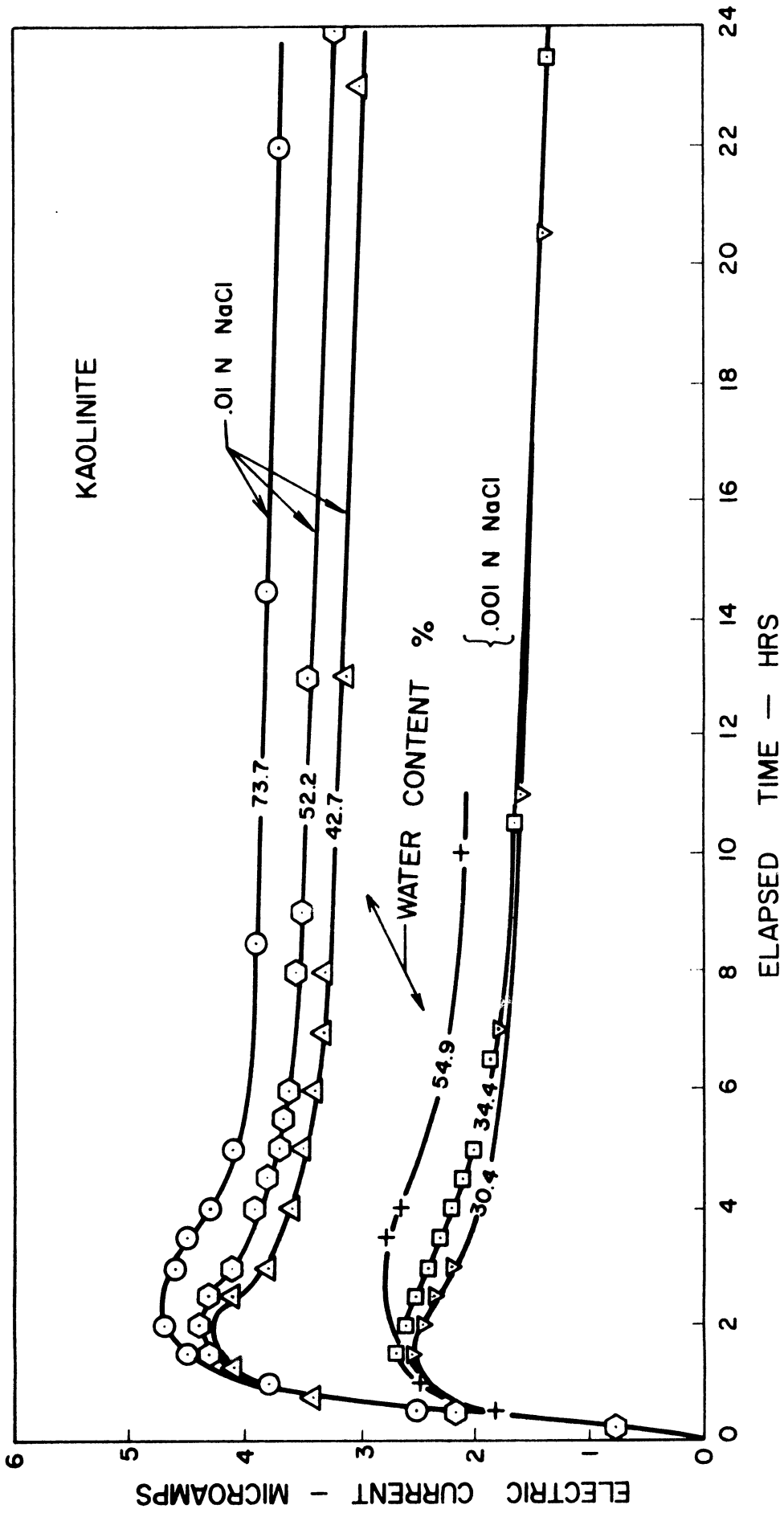


Figure 8. Thermo Electric Current vs. Time in Kaolinite for Various Water Contents and Normality of Saturating Solution. Average Temperature Gradient is 1°C/cm.

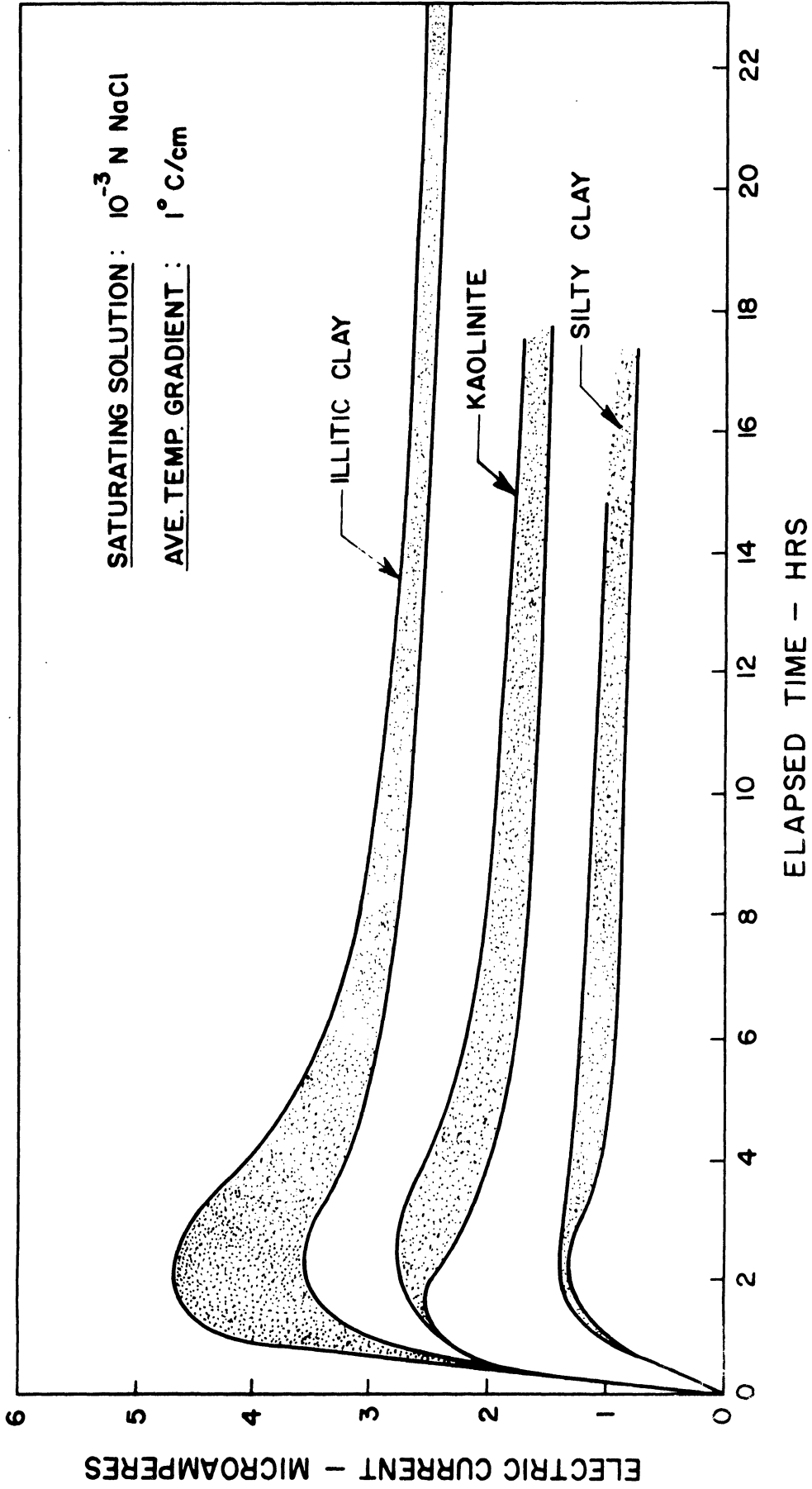


Figure 9. Comparison of Thermo Electric Curve Envelopes for Three Clays.

Typical thermo-electric behavior of the clay-water systems is shown in Figures 8 and 9. The induced thermo-electric current is shown plotted as a function of time for various water contents and pore water electrolyte concentrations in Figure 8. The electric current flow was always from hot to cold, i.e., the hot side had the more positive polarity. The current tended to increase as either the salinity of the saturating solution or the water content was increased. A comparison of the thermo-electric behavior of the three clay systems is shown by a plot of thermo-electric curve envelopes in Figure 9. For a given saturating solution and temperature gradient, the thermo-electric current increased with increasing exchange capacity of the clay.

#### Linearity between Forces and Fluxes

Of considerable interest in this investigation was whether application of a D.C. current or a hydraulic gradient might give non-linear relationships between forces and fluxes. However, linearity of plots was excellent in nearly all cases as shown typically in Figures 4 and 5. Miller (1955) and Cambefort (1961) have aptly described difficulties associated with prolonged electro-osmosis experiments. The intent here is not to minimize the difficulties, but merely to show that reasonable precaution and attention to experimental detail lead to consistent linear results.

#### Validity of Saxen's Law

Saxen's Law was tested over a wide range of water contents - from slurry to solid paste - for several clay-water-electrolyte systems. The results are summarized in the last columns of Tables III and IV.

The equivalence holds quite well in the silty clay and kaolinite but not so well in the illitic clay. In the latter case, however, the deviation occurred mainly at the higher water contents where the clay was still in a slurry form and hence its fabric was more subject to distortion under an applied electrical or hydraulic potential.

Olsen (1965) has recently investigated Saxen's relation in sodium kaolinite consolidated over a range of pressures from 0.5 to 200 kg per sq cm (corresponding roughly to water contents ranging from 60 to 15 per cent). He not only found that the electrokinetic fluxes and forces were strictly linear but also that Saxen's relation was obeyed with a less than one per cent deviation.

It thus appears that Saxen's Law is valid in clay-water systems under a wide range of conditions. This means that existing streaming potential data can be used to predict electro-osmosis.

#### Electro-osmotic Transport vs. Water Content Relationship

Analysis of existing data revealed an interesting relationship between electro-osmotic transport and water content. This relationship is graphically portrayed in Figures 10-14. Olsen's (1961) streaming potential data on sodium clays was converted to its equivalent electro-osmosis form and used to plot these curves. Ballou's (1955) electro-osmosis data on sodium kaolinite and Carr's (1962) data on a collodion membrane are also shown for comparison purposes.

The consistent parabolic shape of the curves in Figures 10 and 11 suggest a relationship between electro-osmotic water transport and water content of the form

$$W = b \left( \frac{\omega}{10} \right)^m \quad (19)$$

where  $W$  = electro-osmotic water transport, moles per Faraday  
 $\omega$  = water content, weight fraction of water  
 $b, m$  = arbitrary constants

If a relationship of the form shown in Equation (19) does exist, then the curves in Figures 10 and 11 should plot as straight lines in logarithmic co-ordinates. Such a plot is shown in Figures 12 and 13 for Olsen's, Ballou's and Carr's data. Electro-osmosis data from the present study is shown plotted in this form in Figure 14. Good linearity of plots is shown in nearly all cases.

In order to make the relationship given in Equation (19) more useful it would be desirable to relate the arbitrary constants 'b' and 'm' to fundamental, easily measured properties of the clay-water-electrolyte system. The constant 'b' is the ordinate intercept and 'm' is the slope of the curves in Figures 12-14. A preliminary correlation between these two constants and the exchange capacity and concentration of the external electrolyte was attempted by Gray (1966). However, additional experimental work is required to test and establish the working limits of such a correlation.



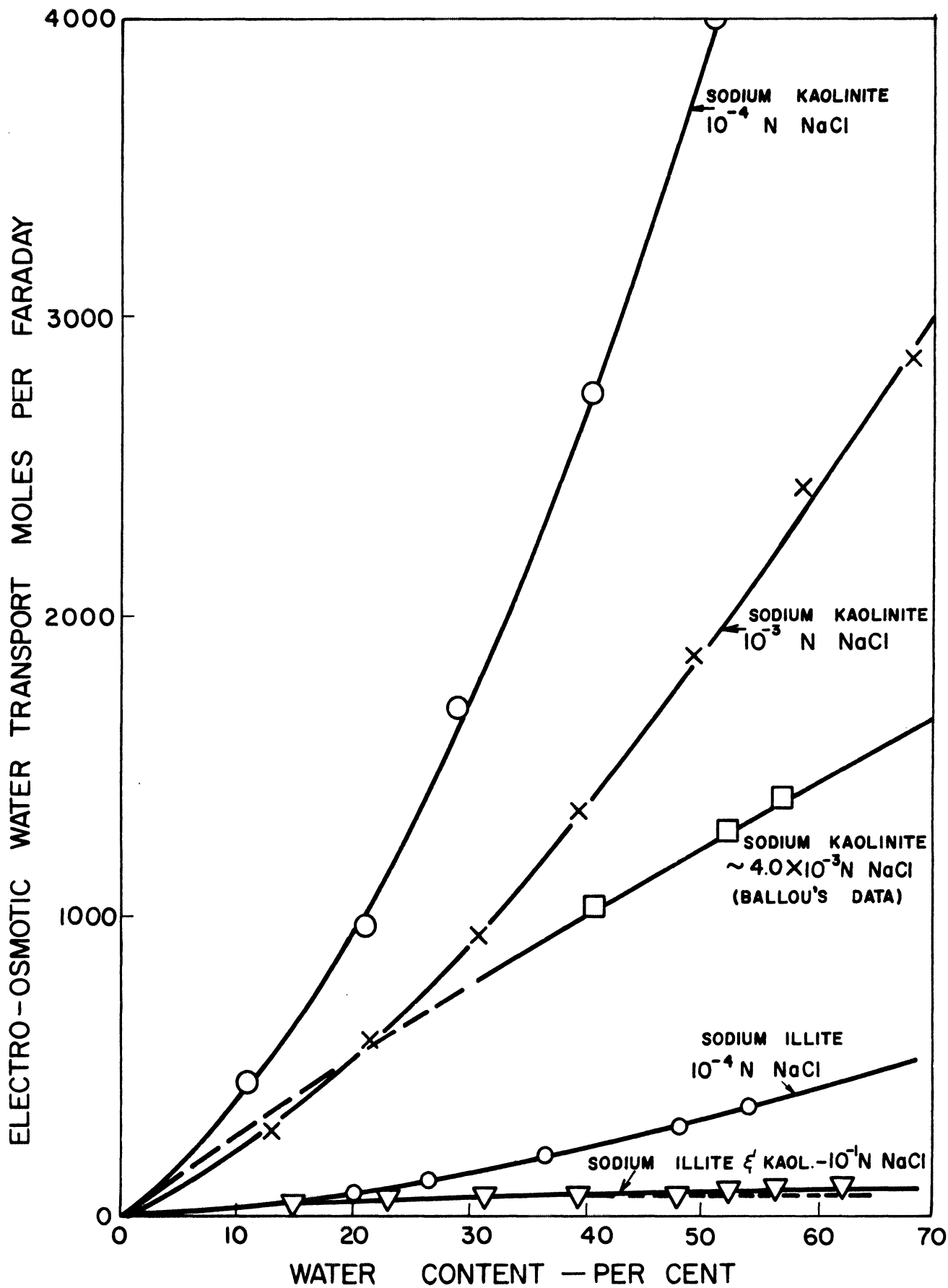


Figure 10. Electro-osmotic Water Transport vs. Water Content for Homoionic Kaolinite and Illite Clays at Various Concentrations of External Electrolyte. (Derived from Streaming Potential Data: Olsen, 1961)

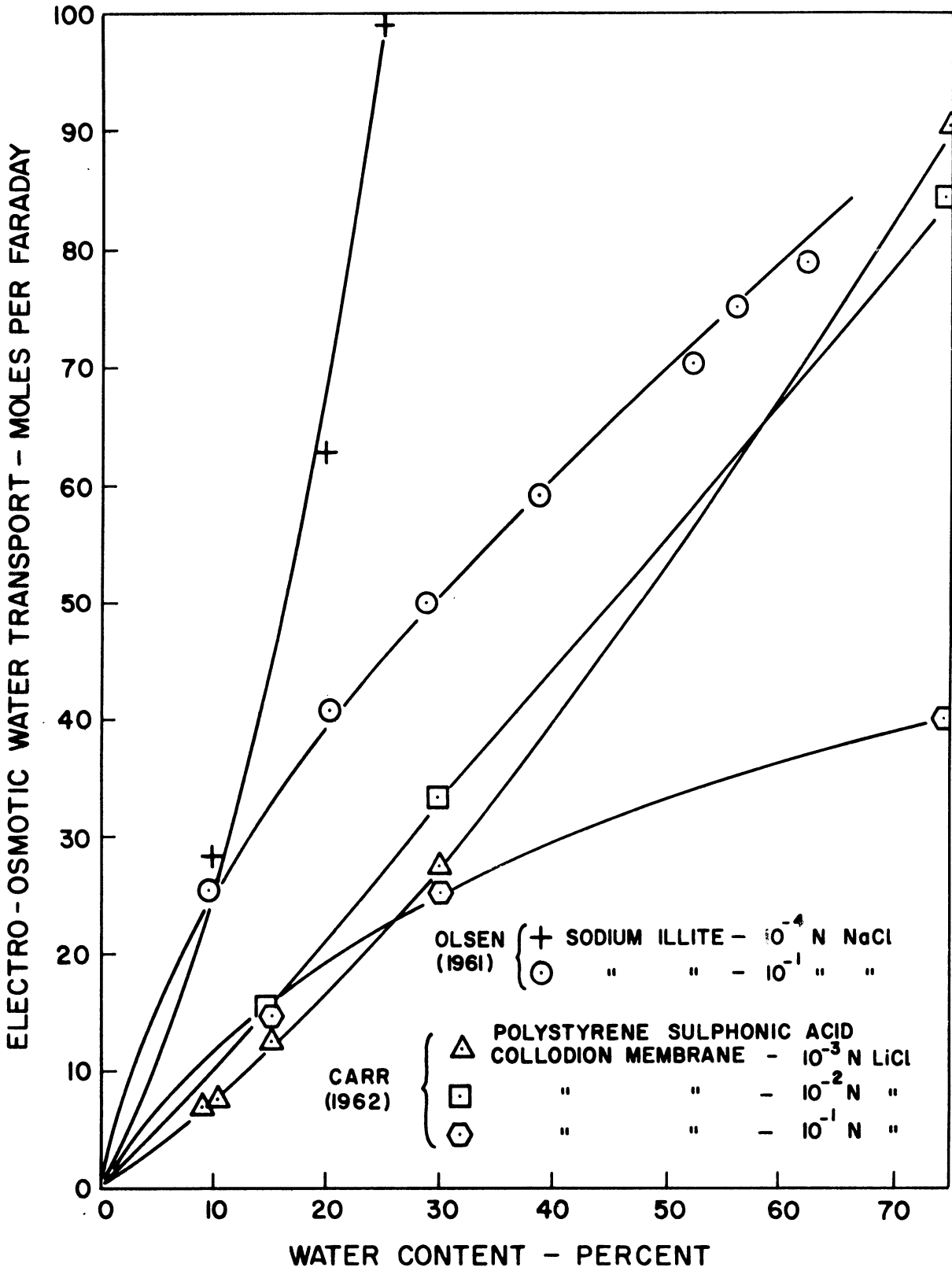


Figure 11. Electro-osmotic Water Transport vs. Water Content for a Sodium Illite Clay and a Polystyrene Collodion Membrane.

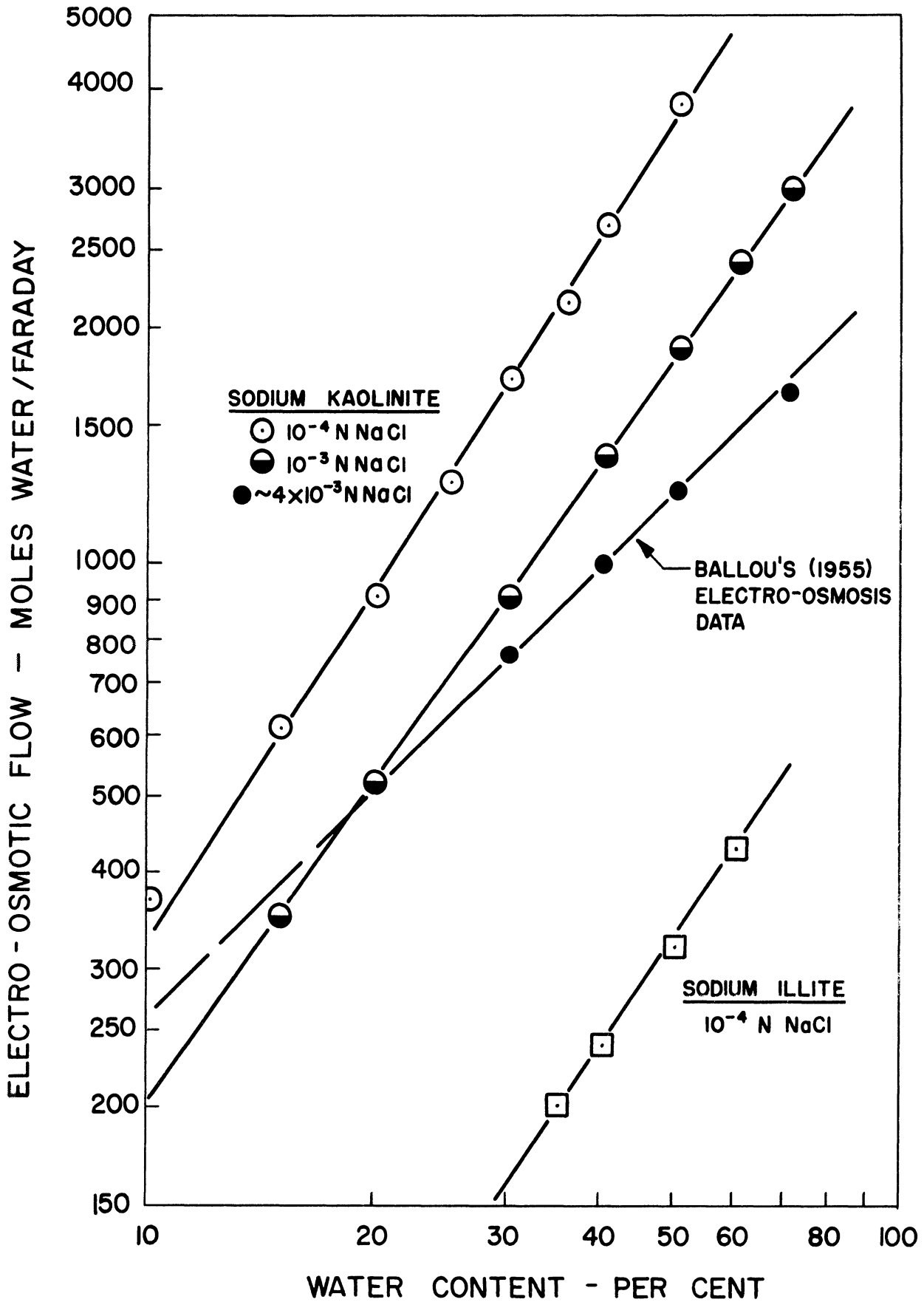


Figure 12. Electro-osmotic Water Transport vs. Water Content for Homoionic Kaolinite and Illite, Plotted in Logarithmic Co-ordinates. (Derived from Streaming Potential Data: Olsen, 1961)

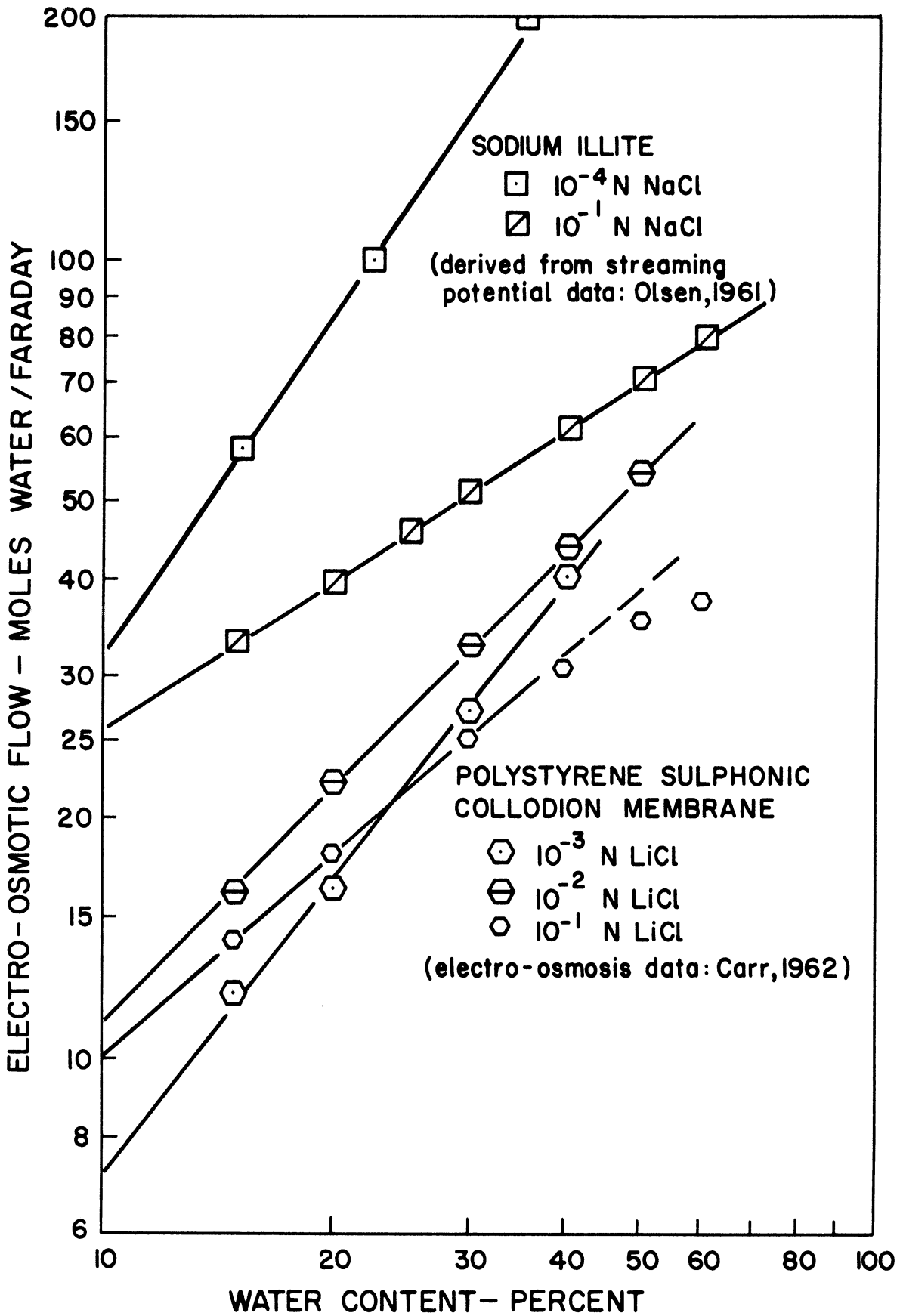


Figure 13. Electro-osmotic Water Transport vs. Water Content for an Illite Clay and a Cationic Collodion Membrane, Plotted in Logarithmic Co-ordinates.

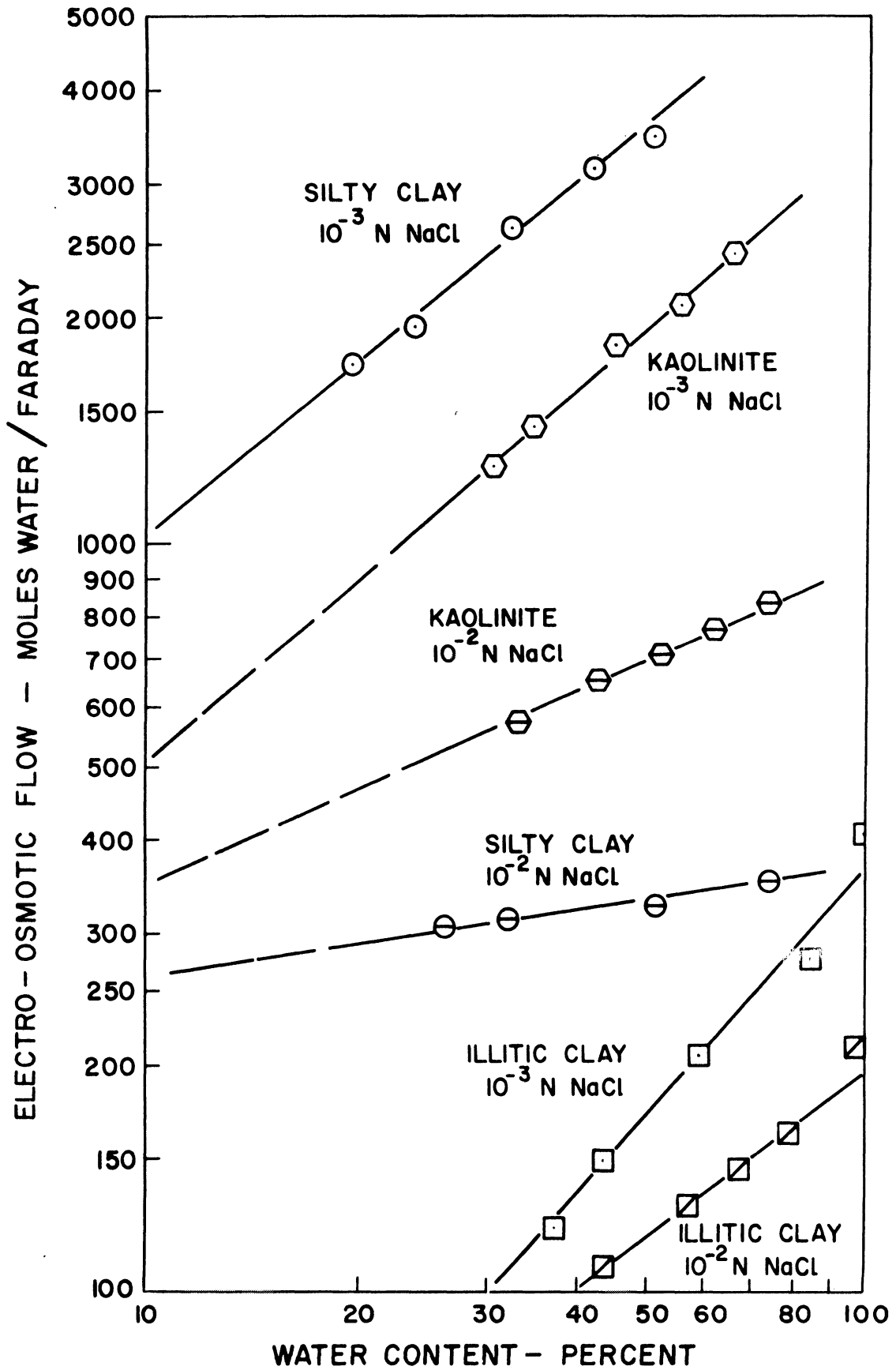


Figure 14. Electro-osmotic Flow vs. Water Content in Clay-Water-Electrolyte Systems, Plotted in Logarithmic Co-ordinates.

## DISCUSSION AND CONCLUSIONS

### Electrokinetic Coupling

The results of this study suggest that electrokinetic processes are controlled mainly by the exchange capacity, the water content, and the concentration of the external electrolyte. A more detailed analysis by Gray (1966) showed that electro-osmosis depends fundamentally on ion distribution and ion selectivity within a porous mass. This dependency can be explained by a general thermodynamic analysis - without involving the kinetic models of Schmid (1951) and Helmholtz (1879).

An interesting relationship between electro-osmotic transport and water content was also observed. This relationship is empirical, but none the less quite remarkable considering its universality, i.e., the wide variety of test data from independent sources and different materials which it fits.

### Thermal Coupling

Whereas the contribution to hydraulic flow from an applied electrical gradient may be considerable, the same cannot be said of thermal gradients in saturated soils. An analysis by Gray (1966) showed that a temperature gradient of at least  $2^{\circ}\text{C}/\text{cm}$  would be required under the most favorable circumstances to produce the same hydraulic flow as a unit hydraulic gradient.

Naturally occurring temperature gradients of  $2^{\circ}\text{C}/\text{cm}$  in the earth are non-existent. This would require, for example, a temperature difference of  $200^{\circ}\text{C}$  over a distance one meter. Natural geothermal gradients in the earth rarely exceed  $3^{\circ}\text{C}$  per 100 feet; one of largest

natural geothermal gradients ever observed is approximately  $6^{\circ}\text{C}$  per 100 feet - the Salton Sea geothermal anomaly, Imperial Valley, California.

The thermal coupling phenomenon of greater practical significance is probably the thermo-electric one. Thermo-electric currents on the order of 1-10 micro amps per  $^{\circ}\text{C}/\text{cm}$  were detected in the clay-water systems. The thermo-electric currents varied in a consistent manner with the water content, exchange capacity, and salinity of the pore water. These currents possibly are significant in electric logging work. They may also contribute to corrosion problems in the ground when a metal casing traverses a geothermal gradient or when metal sheeting surrounds a buried thermal source.

## SUMMARY

Coupling effects arise when a thermodynamic force of one kind induces a flow of another. The forced convection of water through a porous medium, for example, may also cause transfer of electric charge (because ions are carried along in the pore water) which in turn manifests itself as a streaming current or electric potential.

Alternatively, an electric field applied across a porous medium will induce not only a flow of ions in the pore water (normal electrolytic conduction) but also a flow of water due to the drag exerted by the ions on the water molecules. If the number of cations exceeds the number of anions in the pores (the usual case for negatively charged media, e.g., clays and soils), then a proportionately greater drag will be exerted on the water by the cations. Hence, there will be a net flow of water to the cathode in negatively charged media. This phenomenon is known as electro-osmosis; it has been used successfully to dewater and stabilize saturated clays.

Other types of coupling also play an important role in the geologic environment. Temperature and salt concentration gradients across a shale member, for example, may give rise to interesting osmotic and electrical effects. Conventional flow processes and the various coupling effects are summarized in Table I.

In the present study both electrokinetic and thermal coupling phenomena in clays were investigated. Equations based on irreversible thermodynamics were presented which relate the contributions to a given flux, e.g., volume flow, electric current, or heat flow, from various thermodynamic driving forces, viz., pressure, temperature, and voltage.



A theoretical equivalence between coupling coefficients (Onsager's principle) was discussed. This equivalence was investigated experimentally for the electrokinetic case and was shown to be valid in clay-water systems under a wide range of conditions. This means, in effect, that streaming potential data on clay-water systems can also be used to predict the electro-osmotic response of these same systems.

The coupled flows of water, heat, and electricity in saturated clays were experimentally evaluated as the exchange capacity, water content, and concentration of the pore water electrolyte were systematically varied. A linear relationship was observed between electro-osmotic water transport and the logarithm of the water content for a given exchange capacity and external electrolyte concentration. This relationship was valid for both clay-water systems and a collodion membrane.

Measureable thermoelectric currents on the order of a few micro amperes/ $^{\circ}\text{C}/\text{cm}$  were detected in the clay-water systems. The thermoelectric current increased consistently with increasing exchange capacity, water content, or external electrolyte concentration. The warmer side always had a more positive polarity. Thermo-osmotic effects in saturated clay-water systems were also detected, but they were insignificant compared to electro-osmotic contributions to the flow of water in clays.

## REFERENCES

- Ballou, E.V. (1955): Electro-osmotic flow in homoionic kaolinite;  
J. Colloid Science, 10, pp. 450-460.
- Berry, F. and Hanshaw B. (1960): Geologic evidence suggesting membrane properties of shales; 21st Int. Geol. Cong., Abstract Vol., p. 209, Copenhagen.
- Cambefort, H. (1961): Electro-osmose et consolidation electro chimique des argiles; Geotechnique, 11, pp. 203-33.
- Carr, C. W. et al (1962): Electro-osmosis in Ion Exchange Membranes; J. Electrochem. Soc. 109, pp. 251-55.
- Casagrande, L. (1949): Electro-osmosis in soils, Geotechnique, 1, pp. 159-177.
- Casagrande, L. (1953): Review of past and current work on electro-osmotic stabilization of soils; Harvard Soil Mech. Series No. 45, Harvard Univ. Cambridge, Mass.
- DeGroot, S. R., and Mazur, P. (1962): Non-Equilibrium Thermodynamics; North Holland Publ. Co., Amsterdam.
- Denbigh, K. G. (1951): The Thermodynamics of the Steady State: Methuen, London.
- Esrig, M. I. (1964): Report of a feasibility study of electrokinetic processes for stabilization of soils for military mobility purposes; Research Report No. 1 School of Civil Engineering, Cornell University, Ithaca, N. Y.
- Fitts, D. D. (1962): Non-Equilibrium Thermodynamics; McGraw Hill Book Co., New York.
- Goldshtein, M. N. (1959): The thermodynamics of irreversible processes and electro-osmotic transport in disperse systems; Kolloidnyi Zhurnal, 21, no. 1, pp. 30-36.
- Gray, D. H. (1966): Coupled flow phenomena in clay-water systems; Ph.D thesis, University of California, Berkeley.
- Habib, P. and Soeiro, F. (1957): Migrations d'eau dans les sols provoques par une difference de temperature; Proc. 4th Int. Cong. Soil Mech., pp. 40-43.
- Haas, R. and Steinert, C. (1959): Thermo-osmose in Flussig Keiten Messungen. Zeitschrift fur Phys. Chem. Neue Folge., 21, 270-297.

- Helmholtz, H. (1879): \_\_\_\_\_ Ann. Physik. Wied.,  
7, pp. 337.
- Ikeda, T. (1958): Non isothermal membrane potentials, J. Chem. Phys.,  
28, 166.
- Katchalsky, A. and Curran, P. (1965): Non Equilibrium Thermodynamics  
in Biophysics; Harvard University Press, Cambridge, Mass.
- Krischer, O. and Rohnhalter, H. (1940): Wärmeleitung and Dampfdiffusion  
in feuchten Guten. Berlin: VDI Forschungsheft, 402, 1-18.
- Lorenz, P. B. (1952): The phenomology of electro-osmosis and streaming  
potential; J. Phys. Chem., 56, pp. 775-778.
- Lorenz, P. B. (1953): Electro kinetic relations in the quartz-acetone  
system; J. Phys. Chem., 57, pp. 430-434.
- Miller, R. D. (1955): Neglected aspects of electro-osmosis in porous  
bodies; Sci., 122, No. 3165, pp. 373-374.
- Miller, D. G. (1960): Thermodynamics of Irreversible Processes; Chem.  
Revs. 60, pp. 16-37.
- Olsen, H. W. (1961): Hydraulic Flow through Saturated Clays; Ph.D  
thesis, M.I.T.
- Olsen, H. W. (1965): personal communication.
- Marshall, D. J. and Madden, T. R. (1959): Induced Polarization, a  
study of its causes; Geophysics, 24, 790-816.
- Onsager, L. (1931): Reciprocal relations in irreversible processes;  
Phys. Review, 38, 2265-79 and 37, 405-426.
- Prigogine, J. R. (1961): Thermodynamics of Irreversible Processes;  
John Wiley and Sons, New York.
- Saxen, U. (1892): Electrokinetic potentials; Chap. XIV, p. 1225, in  
Textbook of Physical Chemistry by Glasstone, D. Van Nostrand,  
New York.
- Schmid, G: Series of papers in Z. Electrochem.; 54:424 (1950), 55:229  
(1951), 55:684 (1951), 56:35 (1952), 56:181 (1952).
- Spanner, D. C. (1954): The active transport of water under a temperature  
gradient; Symposia of Exp. Biol. VIII, Active Transport,  
pp. 76-93.
- Taylor, S. A. (1963): Simultaneous Flow in Soils and Plants; Utah State  
Univ. Logan.

- Taylor, S. A. and Cavazza, L (1954): The movement of soil moisture in response to temperature gradients, Soil Sci. Soc. Am. Proc., 18, 351.
- Taylor, S. A. and Cary, J. W. (1960): Analysis of the simultaneous flow of water and heat with the thermodynamics of irreversible processes; Trans. Intern. Congr. Soil Sci. 7th Madison. 1:80-90.
- Taylor, S. A. and Cary, J. W. (1964): Linear equations for the simultaneous flow of matter and energy in a continuous soil system; Soil Sci. Soc. Amer. Proc. 28, 167-172.
- Winterkorn, H. P. (1947): Fundamental similarity between electro-osmosis and thermo-osmotic phenomena; HRB Proc., 27, pp. 443-455.
- Winterkorn, H. P. (1955): Water movement through porous hydrophilic systems under capillary, electric, and thermal Potentials; ASTM Symposium on Permeability of Soils, Special Tech. Publ., No. 163, pp. 27-35.